The solid-liquid interfacial free energy out of equilibrium
Supplementary information

Bingqing Cheng

Laboratory of Computational Science and Modeling, Institute of Materials,

École Polytechnique Fédérale de Lausanne, 1015 Lausanne, Switzerland

Gareth A. Tribello

Atomistic Simulation Centre, School of Mathematics and Physics,

Queen's University Belfast, Belfast, BT7 1NN

Michele Ceriotti[*]

Laboratory of Computational Science and Modeling, Institute of Materials,

École Polytechnique Fédérale de Lausanne, 1015 Lausanne, Switzerland

Microscopic and thermodynamic definition of γ_{sl}

In this document we briefly clarify the connections between the atomic-scale simulation of solidification, the thermodynamic definition of a free energy excess for a solid-liquid interface in out-of-equilibrium conditions, and classical nucleation theory.

The central tenet of our treatment is that the thermodynamically consistent way of defining a reference state for a microstate that contains a solid and liquid region separated by an (inevitably) ill-defined interfacial region is to introduce an atom-based order parameter ϕ that distinguishes the solid (with a mean order parameter ϕ_s) from the liquid (average order parameter value ϕ_l). Given the free-energy profile as a function of the total $\Phi = \sum_i \phi(i)$ for a system that is composed of N atoms, one can then define the number of solid atoms in the reference state by inverting the relation $\Phi = n_s \phi_s + (N - n_s)\phi_l$,

$$n_s(\Phi) = \frac{\Phi - N\phi_l}{\phi_s - \phi_l}, \tag{1}$$

This procedure gives you a reference state that has zero surface excess for the order parameter ϕ. The free energy of an idealized system composed of n_s solid atoms and $n_l = N - n_s$ liquid atoms, with no surfaces or interfaces, is equal to $N\mu_l + \mu_{sl}n_s$, where μ_l is the chemical potential of the liquid and μ_{sl} is the difference between the chemical potentials of the solid and liquid. Setting the free energy of the liquid as the reference zero, this leaves us with

$$G(\Phi) = \mu_{sl}n_s(\Phi) + G_{surf}(\Phi) \tag{2}$$

for any system with an interface present. Through this procedure we thus single out an excess term due to the solid-liquid interface.

It is customary to express the surface free energy excess, G_{surf}, as the product of a specific surface energy term γ_{sl} and the area of the interface. The problem in doing so is that there can be some ambiguity in defining the area of the solid region. In our method this problem is circumvented as the area of the interface is defined by the boundary conditions. The biased dynamics is used to trigger the formation of a solid-liquid interface *perpendicular to the elongated direction* of the simulation box. This interface thus has a fixed, total surface area of $A = 2\Delta y \Delta z$. By contrast, in 3D nucleation, both the volume and surface area of the nucleus depend on the definition of the solid region. It is thus not obvious how to factor the surface excess as a product of an area and a nucleus-size-independent γ_{sl} as is required when interpreting nucleation experiments. A model with some assumptions is thus inevitably required. In this model one could take the planar-interface limit of γ_{sl} as a constant, and infer the surface area
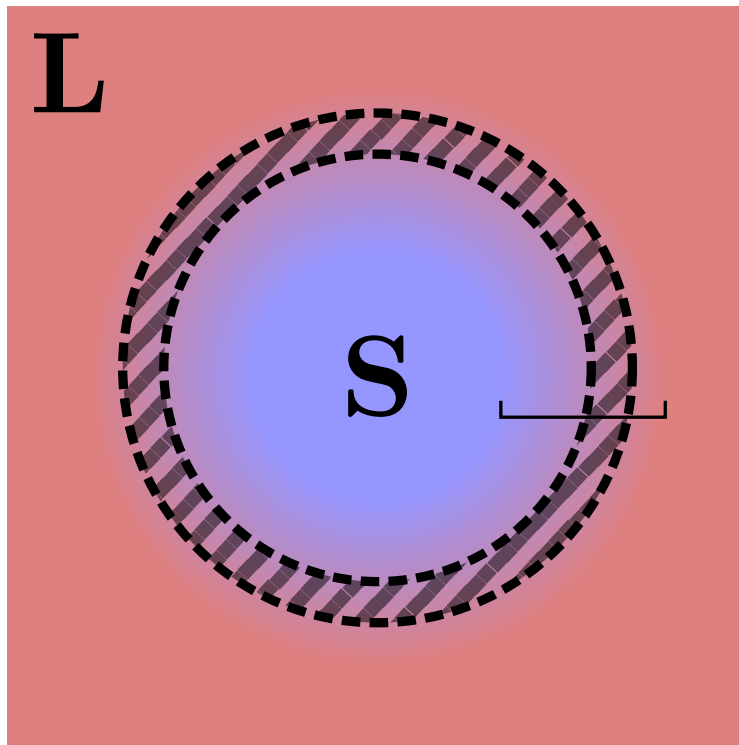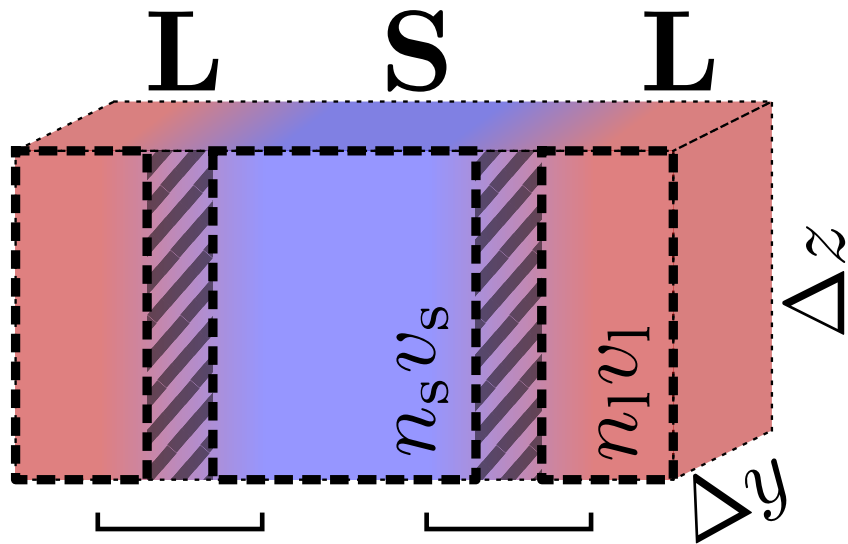
FIG. 1. Schematic representations of the partitioning of simulation cells that are obtained when an order parameter is used to discriminate solid regions from liquid regions. The "excess volume" region is indicated by a dashed pattern. Top: schematic of the boundary conditions of a periodic cell in which there is an idealized, planar-interface simulation. Bottom: geometry for a finite nucleus. Note that the choice of dividing surface changes the volume and surface area of the solid cluster.

of the nucleus from the free energy excess for a given configuration: $\gamma_{sl}A(\Phi) = G(\Phi) - \mu_{sl}n_s(\Phi)$. However, if one instead wanted a predictive model the most common approach is that used in classical nucleation theory (CNT): the surface area of the cluster A is assumed to be related to n_s by $A(n_s) = \sigma n_s^{2/3}$, where σ is a constant that depends on the geometry of the cluster. This implies that the cluster has a fixed shape and a volume proportional to n_s. In setting the proportionality constant, σ, one implicitly assumes that the densities of the solid and liquid portions are fixed. The most natural choice for these fixed densities are the values that would be taken by the bulk solid/liquid under the same thermodynamic conditions. The inverse of these densities are the molar volumes, which we can insert into equation 1 so as to determine $n_s(V)$.

When $n_s(\Phi)$ is defined using an order parameter that is not proportional to the molar volume, the volume of the reference state $n_s(\Phi)v_s + (N - n_s(\Phi))v_l$ (here v_s and v_l are the molar volumes of the bulk solid and liquid) will not equal the actual volume of the system, V. In other words, determining n_s based on Φ makes the volume of the nucleus ill-defined - one could take it to be $n_s(\Phi)v_s$, $V - (N - n_s(\Phi))v_l$, or any intermediate value. Choosing a reference based on the molar volume thus provides the most consistent framework for linking atomic-scale models of nucleation with CNT.

What really matters, however, is how the choice of dividing surface affects the prediction of the free energy of the nucleus, and the activation energy to solidification. As discussed in the main text, for a given configuration of a planar interface in out-of-equilibrium conditions the free energy G is fixed. The choice of order parameter and reference state only affects the way this total energy is partitioned into bulk and interface terms. The specific free energy excesses obtained using two different order parameters ϕ and θ to define the reference state are related by:

$$\gamma_{sl}^{\Theta} - \gamma_{sl}^{\Phi} = -\mu_{sl}\frac{n_s(\Theta) - n_s(\Phi)}{A}. \tag{3}$$

This change in the interfacial free energy can been seen as coming from a shift in the position of the dividing surface along x. As a consequence of this shift, different numbers of atoms are assigned to the solid and liquid parts of the system. Any changes that are observed in the value of γ_{sl} with a different reference state are thus compensated by a change in the bulk term so that the overall free energy of the system remains constant.

A similar treatment also applies in the case of 3D nucleation. Here, however, one has to consider that the choice of reference state will also affect the average density of the solid cluster, i.e. the proportionality constant σ that relates the number of solid atoms to the surface area

of the cluster. For the the overall free energy to be independent of the choice of reference state the following must hold

$$\mu_{\text{sl}} n_{\text{s}}(\Theta) + \gamma_{\text{sl}}^{\Theta} \sigma^{\Theta} n_{\text{s}}(\Theta)^{2/3} = \mu_{\text{sl}} n_{\text{s}}(\Phi) + \gamma_{\text{sl}}^{\Phi} \sigma^{\Phi} n_{\text{s}}(\Phi)^{2/3}. \tag{4}$$

If one assumes that any change in n_{s} is related to the change in surface area by an equation that is analogous to that found in the planar interface limit one can write:

$$n_{\text{s}}(\Phi) - n_{\text{s}}(\Theta) = (\gamma_{\text{sl}}^{\Theta} - \gamma_{\text{sl}}^{\Phi}) \frac{\sigma^{\Phi}}{\mu_{\text{sl}}} n_{\text{s}}(\Phi)^{2/3}. \tag{5}$$

One can then write a relation between σ^{Θ} and σ^{Φ}:

$$
\begin{aligned}
\sigma^{\Theta} &= \sigma^{\Phi} \frac{\gamma_{\text{sl}}^{\Phi} n_{\text{s}}(\Phi)^{2/3}}{\gamma_{\text{sl}}^{\Theta} n_{\text{s}}(\Theta)^{2/3}} + \mu_{\text{sl}} \frac{[n_{\text{s}}(\Phi) - n_{\text{s}}(\Theta)]}{\gamma_{\text{sl}}^{\Theta} n_{\text{s}}(\Theta)^{2/3}} \\
&= \sigma^{\Phi} \frac{\gamma_{\text{sl}}^{\Phi} n_{\text{s}}(\Phi)^{2/3}}{\gamma_{\text{sl}}^{\Theta} n_{\text{s}}(\Theta)^{2/3}} + \sigma^{\Phi} \frac{\left[\gamma_{\text{sl}}^{\Theta} - \gamma_{\text{sl}}^{\Phi}\right] n_{\text{s}}(\Phi)^{2/3}}{\gamma_{\text{sl}}^{\Theta} n_{\text{s}}(\Theta)^{2/3}} \\
&= \sigma^{\Phi} \frac{n_{\text{s}}(\Phi)^{2/3}}{n_{\text{s}}(\Theta)^{2/3}}
\end{aligned}
\tag{6}
$$

One sees that in order to guarantee that CNT results for finite-size nuclei are consistent with the thermodynamic, planar-interface limit, it is necessary to apply a correction to the proportionality constant that relates the solid atom count to the surface area. This scaling ensures that the estimate for the surface area of the cluster is independent of the choice of reference state. Substituting Eq. (5) into Eq. (6) one further time gives

$$\sigma^{\Phi} n_{\text{s}}(\Phi)^{2/3} = \sigma^{\Theta} \left[n_{\text{s}}(\Phi) - \frac{\sigma^{\Phi}(\gamma_{\text{sl}}^{\Theta} - \gamma_{\text{sl}}^{\Phi})}{\mu_{\text{sl}}} n_{\text{s}}(\Phi)^{2/3} \right]^{2/3} = \sigma^{\Theta} n_{\text{s}}(\Phi)^{2/3} \left[1 - \delta\, n_{\text{s}}(\Phi)^{-1/3} \right]^{2/3}, \tag{7}$$

where we introduced the shorthand $\delta = \sigma^{\Phi}(\gamma_{\text{sl}}^{\Theta} - \gamma_{\text{sl}}^{\Phi})/\mu_{\text{sl}}$. Expanding for large $n_{\text{s}}(\Phi)$ gives:

$$\sigma^{\Phi} \approx \sigma^{\Theta} \left[1 - \frac{\delta}{n_{\text{s}}(\Phi)^{1/3}} \right]. \tag{8}$$

Hence, when a different order parameter is used to define the interfacial area, the size-to-area conversion constant that enters the CNT expression for the surface energy must be corrected with a a term $\propto 1/R$. This is formally equivalent to the so-called Tolman correction, which has been shown to be a simple yet effective way to reconcile nucleation rate data obtained for nanoscopic nuclei with results obtained in the planar interface limit [1].

Local order parameter

The local order parameter ϕ for each atom i depends on the position of its nearest neighbors. To single out the first-shell neighbors, we introduce a radial cutoff function between each pair
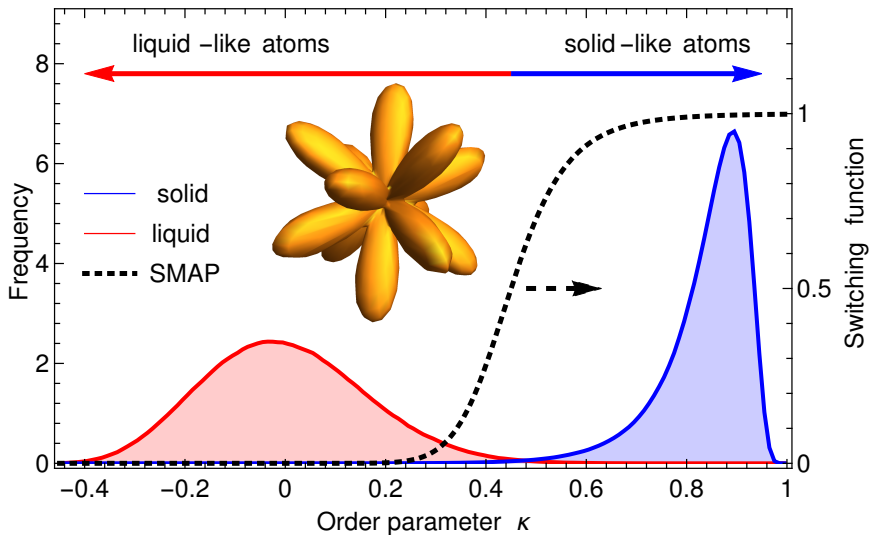
FIG. 2. The distributions of κ for a bulk fcc crystal oriented with the $\langle 100 \rangle$ direction parallel the axes of the simulation cell, and for the bulk liquid. All distributions have been computed at $T = T_{\mathrm{m}}$. SMAP indicates the sketch-map switching function [2] that we used to define $\phi = S(\kappa)$.

of atoms i and j:

$$c_r(r_{ij}) = \begin{cases} 1 & r_{ij} \leq r_1 \\ 0 & r_{ij} \geq r_0 \\ (y-1)^2(1+2y) & r_1 < r_{ij} < r_0 \end{cases} \tag{9}$$

where $y = (r_{ij} - r_1)/(r_0 - r_1)$. We then compute an angular term $c_\alpha(r_{ij})$ to identify whether atom j sits on an fcc lattice point relative to i. This angular term has a functional form inspired by the cubic harmonics

$$c_\alpha(\mathbf{r}_{ij}) = (x^4 y^4 + y^4 z^4 + x^4 z^4)/r_{ij}^8 - a x^4 y^4 z^4/r_{ij}^{12}, \tag{10}$$

Fig. 2 shows the shape of the above cubic harmonic function. The parameter $\alpha = 27$ has been changed from the original value used in Ref. [3]. This new value allows us to differentiate more clearly between different orientations of the fcc environment. This is useful as c_α is not rotationally invariant. It can thus be used in conjunction with a rotation matrix to ensure that an fcc crystal is only detected when it has a particular orientation. This orientation can be specified using a set of Euler angles (ϕ, ψ, θ), i.e.,

$$c_\alpha^{(\phi,\psi,\theta)}(\mathbf{r}_{ij}) = c_\alpha(\mathbf{R}^{(\phi,\psi,\theta)} \cdot \mathbf{r}_{ij}), \tag{11}$$

where

$$\mathbf{R}^{(\phi,\psi,\theta)} = \begin{vmatrix} \cos\phi\cos\psi - \cos\theta\sin\psi\sin\phi & \cos\phi\sin\psi + \cos\theta\cos\psi\sin\phi & \sin\phi\sin\theta \\ -\sin\phi\cos\psi - \cos\theta\sin\psi\cos\phi & -\sin\phi\sin\psi + \cos\theta\cos\psi\cos\phi & \cos\phi\sin\theta \\ \sin\theta\sin\psi & -\sin\theta\cos\psi & \cos\theta \end{vmatrix}. \quad (12)$$

The un-scaled local order parameter κ^0 is then defined as

$$\kappa^0(i) = \frac{\sum\limits_{i \neq j} c_r(r_{ij}) c_\alpha(r_{ij})}{\sum\limits_{i \neq j} c_r(r_{ij})}. \quad (13)$$

This quantity is linearly scaled using $\kappa(i) = (\kappa^0(i) - \kappa_l^0)/(\kappa_s^0 - \kappa_l^0)$ to ensure that the perfect *fcc* lattice corresponds to $\kappa = 1$, while the average κ value for atoms in bulk liquid is zero. The value of $\kappa^0(i)$ in the perfect *fcc* crystal with the desired orientation $\kappa_s^0 = 1/16$ can be readily computed by summing over the positions of the ideal positions of nearest neighbors. It is also possible to analytically integrate the value of $\kappa^0(i)$ in the bulk liquid, as one can safely assume that the distribution of $\mathbf{r}_{ij}$ is uniform in the polar directions, i.e.,

$$\kappa_l^0 = \int_0^\pi \mathrm{d}\theta \int_0^{2\pi} \mathrm{d}\phi \, c_\alpha(r_{ij}(\phi,\theta,r=1)) = \frac{143-a}{5005}. \quad (14)$$

For a given choice of a, $\kappa(i) = \frac{80080}{2717+16a}\kappa^0(i) + \frac{16(a-143)}{2717+16a}$.

Figure 2 shows that the atoms in bulk *fcc* crystal and bulk liquid have a minimal amount of overlap in the distribution of the local order parameter κ. Consequently, a tunable sigmoid switching function [4] can be used to map each atom onto the solid-like or the liquid-like regime, i.e.,

$$\phi(i) = S(\kappa(i)) = 1 - (1 + (2^{a/b} - 1)(\kappa(i)/R_0)^a)^{-b/a}, \quad (15)$$

The switching function used in this work is shown in figure 2. It has $a = 8$, $b = 8$, and $R_0 = 0.45$. These values were selected so that $\phi = 0.5$ corresponds to the crossover point at which the κ distributions for the atoms belonging to the bulk crystal and the bulk liquid cross.

Simulation details

A truncated Lennard-Jones potential was used [5–7]:

$$u(r) = \begin{cases} 4\epsilon\left[\left(\frac{\sigma}{r}\right)^{12} - \left(\frac{\sigma}{r}\right)^6\right] + C_1 & r \leq 2.3\sigma \\ C_2\left(\frac{\sigma}{r}\right)^{12} + C_3\left(\frac{\sigma}{r}\right)^6 + C_4\left(\frac{\sigma}{r}\right)^2 + C_5 & 2.3\sigma < r < 2.5\sigma \\ 0 & r \geq 2.5\sigma \end{cases} \quad (16)$$

where $C_1 = 0.016132\epsilon$, $C_2 = 3136.6\epsilon$, $C_3 = -68.069\epsilon$, $C_4 = -0.083312\epsilon$, and $C_5 = 0.74689\epsilon$. The time step was set equal to 0.004 Lennard-Jones time units, which gives negligible drift in the conserved quantities for this system. The NPT ensemble was employed throughout with the Nose-Hoover thermostat and barostat used to control the temperature and pressure. Only the x dimension of the supercell was allowed to fluctuate under the barostat. The y and z dimensions of the simulation cell were set so that they were commensurate with the equilibrated lattice at the appropriate simulation temperature.

For the simulation runs presented in Figures 1 and 2 in the main text, a supercell with 5184 atoms was used. The total number of steps in each run was set equal to 5×10^7. In order to reduce the total simulation time, the simulations in Figure 3 were performed using a smaller supercell containing 1200 atoms or 1152 atoms for the $\langle 100 \rangle$ and $\langle 111 \rangle$ lattice directions respectively. In addition, during these runs the system was restrained so that it remained in a state that was somewhere between partially-solid/partially-liquid and completely solid. This choice allows us to converge the free energy profiles much more quickly because the system never fully melts, and a surface with the proper orientation is always available to promote solidification. Since one can infer the value of μ_{sl} from the slope of the plateau region in the free energy profile, it is still possible to extract an estimate of $\gamma_{\mathrm{sl}}(T)$. We have meticulously checked the finite-size effects on γ_{sl} for this simulation box size, and confirmed that when γ_{sl} is computed in this way it is well-converged with respect to the results from simulations of larger box sizes with complete melting. The simulation length for each run in Figure 3 was 2×10^7 time steps.

The PLUMED plug-in adds a bias potential to the system Hamiltonian. The metadynamics bias and other constraints are calculated and updated inside the PLUMED software. At each step of the simulation, the PLUMED software receives the atomic configuration from LAMMPS, computes local order parameters and global collective variables, and returns an external bias potential to the MD code.

In the following pages, sample input files for simulations performed with the interface in the $\langle 111 \rangle$ direction in Figure 3 are provided.

Sample LAMMPS input file

Here is a sample LAMMPS input file for running the molecular dynamics simulations of the solid-liquid systems.

```
atom_style      atomic
units           lj
```

```
dimension      3
boundary       p p p
processors     * * 1


read_data      ./data.lj   # Coordinate file
```

Atoms of type 1 are the Lennard-Jones particles with the truncated pairwise potential [5–7]. The atom of type 2 is a fixed ghost atom that does not interact with its surroundings. It is used as reference point in some of the collective variables.

```
group real type 1
velocity real create 0.6 RandomSeedHere dist gaussian


pair_style table linear 5000
pair_coeff 1 1 tr-lj.table TR_LJ 2.5
pair_coeff * 2 tr-lj.table NULL 2.5


neighbor       1.0 bin


timestep 0.004
```

An initial equilibration of 20'000 steps is performed before starting the biased dynamics. During this equilibration a highly efficient Generalized Langevin thermostat [8] is employed.

```
fix 1 real press/berendsen x 0.0 0.0 1.0
fix 2 real gle 6 0.60 0.60 RandomSeedHere smart2.A every 5
run 20000   # Equilibration time
unfix 1
unfix 2
```

After the equilibration a metadynamics simulation in the NPT ensemble, using a Nosé-Hoover barostat and thermostat is started. Only the elongated axis of the cell is left free to fluctuate. 20 million steps are performed for each simulation.

```
fix 3 real npt temp 0.60 0.60 0.2 x 0.0 0.0 0.5
fix 4 all plumed   plumedfile  plumed.dat     outfile p.log


thermo 500
thermo_style one
dump coord all xyz 5000 traj.xyz


run             20000000
write_restart restart.lj
```


Sample PLUMED input file

Here we provide a sample input file for PLUMED. This input was used to compute the surface free energy excess for the γ_{111} surface. In addition to returning the metadynamics bias potential that promotes the solid-liquid transitions, this PLUMED input also defines a number of restraint potentials that ensure that the central region of the supercell remains in the solid, *fcc* structure.

```
UNITS NATURAL
RESTART
```

Record the volume of the simulation cell.

```
cell: CELL
```

We first compute the local order parameter κ using the cubic harmonic function "FCCUBIC". "ALPHA" specifies the value of the a parameter in Eqn. 10. "PHI", "THETA" and "PSI" define the three Euler angles in Eqn. 12. By specifying these Euler angles we ensure that the CV only identifies atoms as being in an fcc crystals if the $\langle 111 \rangle$ lattice direction is along the x axis of the system. The sigmoid switching function "SMAP" is used to do a non-linear mapping on κ as described in Eqn. 15. We collect $\Phi = \sum S(\kappa(i))$ - the global order parameter used to identify n_s^Φ - using the keyword "MORE_THAN". The value of "cub.morethan" is proportional to the number of atoms in the fcc crystal with the specified lattice direction.

The system contains a total of 1152 real atoms, The 1153th atom is a "ghost" atom that stays stationary at the center of the supercell. This ghost atom is only used as a reference point and allows us to indicate the relative positions of the atoms in some CVs.

```
FCCUBIC ...
LABEL=cub
SPECIES=1-1152 SWITCH={CUBIC D_0=1.2 D_MAX=1.5}
MEAN
MORE_THAN={SMAP R_0=0.45 D_0=0.0 A=8 B=8}
ALPHA=27 PHI=-1.5708 THETA=-0.61548 PSI=0.785389
... FCCUBIC
```

At undercooled conditions, the system has a strong tendency to form solids. Although the central region of the supercell is constrained to remain as an fcc crystal with the $\langle 111 \rangle$ lattice direction along the x axis of the system, the peripheral region is likely to form twinned crystals or mis-oriented crystals with grain boundaries. As the local order parameter κ is not rotational-invariant, any atoms in wrongly orientated crystals usually adopt values intermediate between those obtained for bulk solid and liquid. These crystals with unwanted orientations will be misidentified as partially liquid, and will be included in the computed free energy profile. When this happens, the free energy profile shows bumps as in Ref. [3], which hinders the determination of μ_{sl} and γ_{sl}. For this reason, "cub2", "cub3", "cub4" and "cub5" are used to identify fcc crystals with unwanted orientations. Constraints are added on these CVs to prevent the formation of solid phase with an orientation incompatible with the simulation box.

```
FCCUBIC ...
LABEL=cub2
SPECIES=1-1152 SWITCH={CUBIC D_0=1.2 D_MAX=1.5}
MORE_THAN={SMAP R_0=0.05 D_0=0.4 A=16 B=8}
ALPHA=27 PHI=-1.5708 THETA=0.61548 PSI=2.35619
... FCCUBIC
```

```
FCCUBIC ...
LABEL=cub3
SPECIES=1-1152 SWITCH={CUBIC D_0=1.2 D_MAX=1.5}
MORE_THAN={SMAP R_0=0.05 D_0=0.4 A=16 B=8}
ALPHA=27 PHI=1.5708 THETA=-1.29515 PSI=0.785389
... FCCUBIC
```

```
FCCUBIC ...
LABEL=cub4
SPECIES=1-1152 SWITCH={CUBIC D_0=1.2 D_MAX=1.5}
MORE_THAN={SMAP R_0=0.05 D_0=0.4 A=16 B=8}
ALPHA=27 PHI=-0.2014 THETA=1.84644 PSI=1.71269
... FCCUBIC
```

```
FCCUBIC ...
LABEL=cub5
SPECIES=1-1152 SWITCH={CUBIC D_0=1.2 D_MAX=1.5}
MORE_THAN={SMAP R_0=0.05 D_0=0.4 A=16 B=8}
ALPHA=27 PHI=-0.61548 THETA=-1.5708 PSI=-0.785398
... FCCUBIC
```

The 1153th ghost atom is used as a landmark. These commands allow us to calculate the value of the order parameter in the central slice of the box, in the side regions and in the border slice of the supercell. Notice that the sigmoid switching function "SMAP" in Eqn 15 is tuned in order to facilitate the biasing procedures.

```
centercub: AROUND DATA=cub ATOM=1153 XLOWER=-1.2 XUPPER=1.2 SIGMA=0.5 MORE_THAN={SMAP R_0=0.5 D_0=0.0 A=8 B=8}
sidecub: AROUND DATA=cub ATOM=1153 XLOWER=-2.3 XUPPER=2.3 SIGMA=0.5 OUTSIDE LESS_THAN={SMAP R_0=0.5 D_0=-0.1 A=8 B=2}
bordercub: AROUND DATA=cub ATOM=1153 XLOWER=-7.0 XUPPER=7.0 SIGMA=0.5 OUTSIDE LESS_THAN={SMAP R_0=0.5 D_0=-0.45 A=8 B=8}
```

Well-tempered metadynamics is used to induce transitions between the liquid and the *fcc* crystal for the region on the side of the supercell. An external history-dependent bias potential is gradually accumulated in the space of the CV "sidecub.lessthan". A Gaussian that should cover the space of 600 timesteps in the CV space is deposited every 1600 time steps, with the maximum height equal to 0.15 Lennard-Jones energy unit. The well-tempered option is activated with the biasfactor set to 90.

```
METAD ...
LABEL=metad
ARG=sidecub.lessthan
PACE=1600 HEIGHT=0.15 SIGMA=600 FILE=HILLS
TEMP=0.60 BIASFACTOR=90
ADAPTIVE=DIFF SIGMA_MAX=50 SIGMA_MIN=0.1
... METAD
```

A restraint is used to keep the central slice of the simulation cell, near to the ghost atom, crystalline.

```
wall: LOWER_WALLS ARG=centercub.morethan AT=140 KAPPA=2.0
```

Several restraints are added to prevent nucleation of crystals with unwanted crystal orientations.

```
notwin2: UPPER_WALLS ARG=cub2.morethan AT=14 KAPPA=0.4
notwin3: UPPER_WALLS ARG=cub3.morethan AT=14 KAPPA=0.2
notwin4: UPPER_WALLS ARG=cub4.morethan AT=14 KAPPA=0.2
notwin5: UPPER_WALLS ARG=cub5.morethan AT=14 KAPPA=0.1
```

A further bias is added on the atoms at the border of the simulation box far away from the ghost atom, in order to facilitate the nucleation of the melt starting from the edge of the supercell.

```
softliquid: LOWER_WALLS ARG=bordercub.lessthan AT=30 KAPPA=0.005
```

Finally the instantaneous values of the CV and the biases are recorded. These are used in the re-weighting processes to construct the FES, e.g.

$$G(\Phi) = -\frac{1}{\beta} ln \left(\frac{\int dt e^{\beta V_{tot}(t)} \delta(\Phi)}{\int dt e^{\beta V_{tot}(t)}} \right), \tag{17}$$

where $\beta = 1/k_{\mathrm{B}}T$, and $V_{tot}(t)$ is the total external bias including the metadynamics bias and the restraint biases at time t.

```
PRINT STRIDE=10
ARG=cell.ax,cub.* ,metad.bias,wall.bias,notwin2.bias,notwin3.bias,notwin4.bias,notwin5.bias,softliquid.bias FILE=FES

PRINT STRIDE=10
ARG=cub2.*,cub3.*,cub4.*,cub5.*,centercub.*,sidecub.*,sidecub.* ,bordercub.*  FILE=COLVAR

ENDPLUMED
```

* michele.ceriotti@epfl.ch

[1] S. Prestipino, A. Laio, and E. Tosatti, Phys. Rev. Lett. **108**, 1 (2012).

[2] M. Ceriotti, G. A. Tribello, and M. Parrinello, Proceedings of the National Academy of Sciences **108**, 13023 (2011).

[3] S. Angioletti-Uberti, M. Ceriotti, P. D. Lee, and M. W. Finnis, Physical Review B **81**, 125416 (2010).

[4] M. Ceriotti, G. A. Tribello, and M. Parrinello, Proc. Natl. Acad. Sci. USA **108**, 13023 (2011).

[5] R. L. Davidchack and B. B. Laird, The Journal of chemical physics **118**, 7651 (2003).

[6] S. Angioletti-Uberti, M. Ceriotti, P. D. Lee, and M. W. Finnis, Phys. Rev. B **81**, 125416 (2010).

[7] R. Benjamin and J. Horbach, The Journal of chemical physics **141**, 044715 (2014).

[8] M. Ceriotti, G. Bussi, and M. Parrinello, J. Chem. Theory Comput. **6**, 1170 (2010).